

An Extension of the Oliver and Pharr Method to Ultra-Thin Structures, Coatings, Functionally Graded Coatings and Multilayer Systems

Norbert Schwarzer, Saxonian Institute of Surface Mechanics
Lieschow 26, 18569 Ummanz / Rügen, Germany, info@siomec.de, www.siomec.de

Abstract

It is well known that the classical Oliver and Pharr method is based on a theoretical approach for linear elastic monolithic (homogeneous) half spaces only. Thus, in the case of nanoindentation experiments in coated materials, the problem arises of how to correctly take the substrate effect, the foundation and other underlying structures (like transition areas at the interface) into account. Already 12 years ago Bolshakov, Oliver and Pharr gave the answer to this problem by introducing the “**Concept of the Effective Indenter**”, even though they did not claim it as the solution to the above mentioned problem. Only it was rather difficult to build up a complete theoretical apparatus for this concept and to incorporate it into a sufficiently handy software package. This short documentation will introduce the new concept of Pharr and its powerful potentials in treating problems the classical Oliver and Pharr method can not deal with properly.

Introduction

As it is a well established fact, that the classical Oliver and Pharr method [1], as an approach based upon the half space model, cannot directly be applied to layered materials and small structures, the author here refers to the literature [e.g. 2]. Already in 1995 [3] George Pharr introduced the “Concept of the Effective Indenter” and refined it in a series of wonderful publications until in 2002 the paper about “Understanding of nanoindentation unloading curves” [4] was published. During a small conference in Italy in 1999, the author learned of the concept and promised Pharr, who called his idea the “Funny Indenter Concept” those days, to work out a theory solving not only the problem for the mechanical contact of an indenter with general shape of symmetry of revolution, but also to extend this solution to layered structures. Soon, however, he forgot about this idea and his promise, too. It was brought back into his mind after George Pharr silently handed him a copy of his “understanding-paper” in summer 2003 and slightly embarrassed by his lack of dependability the author finally started working on the problem and published its solution in 2004 [5]. Later on he also presented a variety of applications together with Pharr, Chudoba and Richter [6 - 10]. As a rather stubborn theoretician however, the author needed another “push” from Professor Pharr before he realised that the

“effective indenter theory”, even though powerful, was not something one could easily give to the engineer or an indenter experimentalist and expect him to use it as a tool for the analysis of indentation data. The reason for this is the complexity of the formulae building up the solution. So, with the help of his lovely wife, two faithful programmers and a highly committed web-designer the author succeeded in bringing the whole approach into the software package FilmDoctor®. Within this short note its application on previously published nanoindentation results [11] into a very thin film of only 44nm will be demonstrated.

Theory for effective indenters

In order to have a sufficiently great variability for the definition of differently shaped “effective indenters”, we apply the extended Hertzian approach as shown for example in [12]. With this approach normal and even tangential load distributions of the form [5]

$$\sigma_{zz0}(r, \varphi) = \sum_{n=0}^N c_{\sigma n} r^n \sqrt{a^2 - r^2} \quad (1)$$

$$\begin{aligned} \tau_{rz0}(r, \varphi) &= \sum_{n=0}^N c_{\tau rn} r^n \sqrt{a^2 - r^2} \\ \tau_{xz0}(r, \varphi) &= \sum_{n=0}^N c_{\tau xn} r^n \sqrt{a^2 - r^2} \\ \tau_{yz0}(r, \varphi) &= \sum_{n=0}^N c_{\tau yn} r^n \sqrt{a^2 - r^2} \end{aligned} \quad (2)$$

with $n=0,2,4,6$ and arbitrary constants c (and by following the instructions of the mathematical procedures for obtaining the complete potential functions as given in [5] even arbitrary high but only even N) can be solved completely.

Together with lateral loads (occurring in all tribotesters plus the next generation of nanoindenters and their application see e.g. [12]) one often faces tilting moments leading to a normal surface stress distribution of the form

$$\sigma_{zz0}(r, \varphi) = \sum_{n=0}^N c_{\sigma n} r^{n+1} \cos(\varphi) \sqrt{a^2 - r^2} \quad (3)$$

These stresses can for example occur when the indenter shaft is dragged over the surface. Because the shaft itself is elastic and thus would be bent during the lateral loading, an unavoidable tilting

moment results and acts on the contacted surface. Also curved surfaces (e.g. due to roughness) can lead to such tilting moments.

A defect model: Tool for the construction of relatively general intrinsic stress distributions caused by internal inhomogeneities

In order to simulate the internal complex material structure of porous or composite materials, certain

$$\tau_{rz0}(r_i = \sqrt{(x-x_i)^2 + (y-y_i)^2}, z_i + 0) = \sum_{n=0}^N c_{\tau i,n} r_i^n \sqrt{a_i^2 - r_i^2}$$

$$\tau_{rz0}(r_i = \sqrt{(x-x_i)^2 + (y-y_i)^2}, z_i - 0) = -\sum_{n=0}^N c_{\tau i,n} r_i^n \sqrt{a_i^2 - r_i^2}$$
(4)

$$\sigma_{zz0}(r_i = \sqrt{(x-x_i)^2 + (y-y_i)^2}, z_i + 0) = \sum_{n=0}^N c_{\sigma i,n} r_i^n \sqrt{a_i^2 - r_i^2}$$

$$\sigma_{zz0}(r_i = \sqrt{(x-x_i)^2 + (y-y_i)^2}, z_i - 0) = -\sum_{n=0}^N c_{\sigma i,n} r_i^n \sqrt{a_i^2 - r_i^2}$$
(5)

(with x_i, y_i, z_i denoting the centre of the defect and $n=0,2,4,6$) directly allows us the application of the extended Hertzian approach [5] that provides a complete solution of the elastic field of the defect loading given above. By superposing a multitude of such “defect dots”, one could model (simulate) a very great variety of material inhomogeneities and intrinsic stress distributions. The evaluation of the complete elastic field is straight forward. It only requires the evaluation of certain derivatives of the potential functions given in [5].

Finally, we need to take into account the curvature of the surfaces in order to their effect on the resulting contact pressure distribution [13]. As the theoretical approach would not find enough space in this short note, the author will publish the necessary details elsewhere. However, the interested reader may derive the results presented here by comparing the solutions of the Laplace equation in Cartesian and Paraboloidal coordinates.

Modelling Results: An Example

layer	W	E	ν	h
layer 1	0.17	165	0.23	0.044
layer 2	0.25	165	0.23	
layer 3	0.33	165	0.23	
layer 4	0.41	165	0.23	
layer 5	0.49	165	0.23	
layer 6	0.57	165	0.23	
layer 7	0.65	165	0.23	
layer 8	0.73	165	0.23	
layer 9	0.81	165	0.23	
layer 10	0.89	165	0.23	
substrate	∞	165	0.23	

Fig. 1: Material definition page [14]. The coating, with its Young's modulus yet unknown, is given the substrate Young's modulus as starting or dummy-parameter.

As an example for the extension of the classical Oliver and Pharr method we here investigate a 50μN-ACCU-tip indenter (very sharp Berkowich tip) into a 44nm-TiN-coating as performed by Chudoba et al [11]. The first step is to evaluate the effective indenter to the unloading curve shown in fig. 2. By

defect fields must be developed and combined with the external loads. Circular disc-like inclusions could for example be simulated by the use of plane defects within the layered half space. So, introducing circular defects of radii a_i of the loading type:

using the software package FilmDoctor and applying the automated fitting procedure the thing could be done in a very comfortable manner. However, in order to show the principles of this procedure, we here demonstrate it with an effective sphere “fitted by hand”.



Fig. 2: Choosing “fit load-depth curve” from the load definition methods tree.

We apply the “effective indenter concept” as some kind of add-on to the classical Oliver and Pharr method by using the results of the latter as starting values for our procedure. So, after defining our layered material (fig. 1) with the known substrate parameters and the coating thickness of 44nm, we choose the tool “fit load-depth curve” from the load definition window (fig. 2).

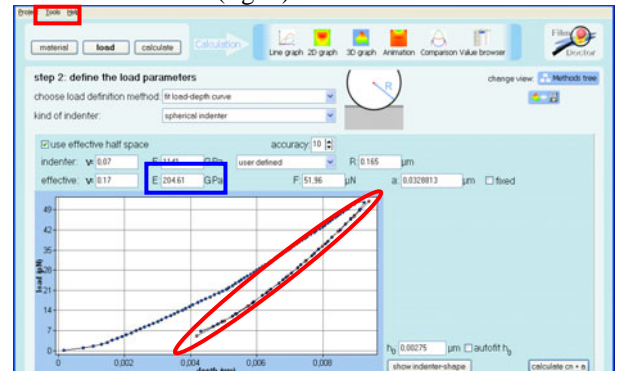


Fig. 3: Fitting an effective spherical indenter to the unloading curve and applying the results from the classical Oliver and Pharr method as starting parameters. Here also

an automated fitting procedure could be chosen with higher accuracy and flexibility (arbitrary paraboloid).

After typing in the Young's modulus of the equivalent half space as this was determined by the Oliver and Pharr method (here 204.61GPa – blue rectangle in Fig. 2), we seek an effective sphere with a radius of curvature $R=165\text{nm}$ fitting the unloading curve.

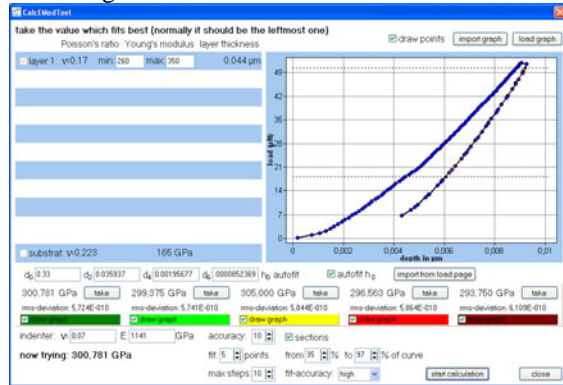


Fig. 4: Fitting a coating Young's modulus to the unloading curve by using the effective sphere of fig. 3.

After that we select the module "CalcEModTool" from the tool box menu (red rectangle in fig. 3), import the load-depth curve and the effective sphere from the "fit load-depth curve" window (fig. 4) and start the evaluation of the coating Young's modulus for the previously found effective indenter. The average result of approximately $326\text{GPa} \pm 35\text{GPa}$ for a variety of fit ranges used from the unloading curve is in good agreement with the surface acoustic wave (339 ± 4) and the elastic indentation (333 ± 25) measurements presented in [11].



Fig. 5: Material definition page. Now we can type in the evaluated coating Young's modulus.

Now we can use this evaluated Young's modulus of the coating (fig. 5) and calculate the complete stress field in the moment of maximum load (fig. 6).

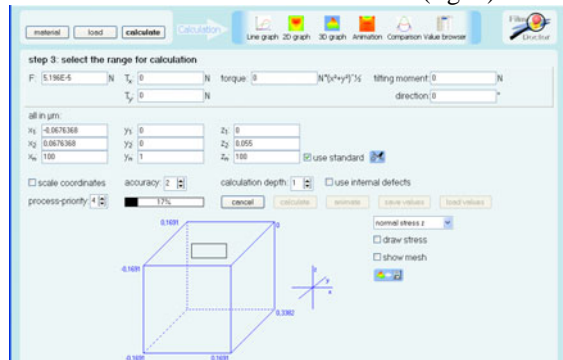


Fig. 6: Calculation page. Within a few seconds the complete stress field with 28 elastic field components can be evaluated for the moment of beginning unloading of our 44nm-coating-substrate system.

Fig. 7 shows the von Mises stress. As we know that due to Oliver&Pharr's concept of completely elastic unloading the plastic flow must just have stopped in the moment of beginning unloading, we take the von Mises maximum as the yield strength Y of the coating material. We find the value to be in good agreement with the yield strength one also would expect from this material [8].

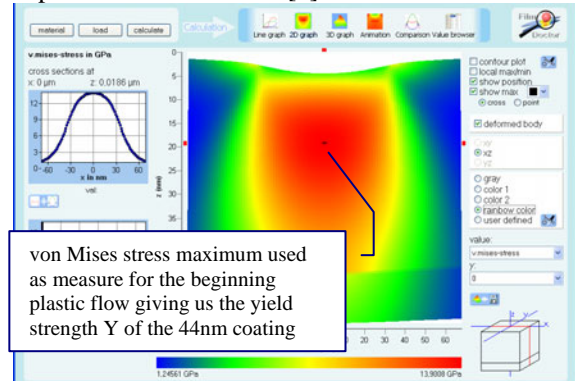


Fig. 7: 2D view of the v. Mises stress in the moment of beginning unloading of our 44nm-coating-substrate system.

References

- [1] W.C. Oliver and G.M. Pharr, J. Mater. Res. 7, 1564 (1992)
- [2] T. Chudoba, K. Herrmann, Härtereitechnische Mitteilungen, HTM 56 (2001) 258
- [3] A. Bolshakov, W.C. Oliver, and G.M. Pharr, MRS Symp. Proc 356, p675 (1995)
- [4] Pharr GM, Bolshakov B (2002) Understanding nanoindentation unloading curves, J. Mater. Res., Vol. 17, No. 10, Oct 2002
- [5] N. Schwarzer, J. Phys. D: Appl. Phys., 37 (2004) 2761-2772
- [6] N. Schwarzer, G. M. Pharr, Thin Solid Films, Vol. 469-470C pp. 194-200
- [7] N. Schwarzer, T. Chudoba, G. M. Pharr, Surf. Coat. Technol, Vol. 200/14-15 pp 4220-4226
- [8] N. Schwarzer, T. Chudoba, F. Richter, Surf. Coat. Technol., Vol 200/18-19 pp 5566-5580
- [9] N. Schwarzer, Thin Solid Films 494 (2006) 168 – 172
- [10] N. Schwarzer, Phil. Mag. 86(33-35) 21 Nov - 11 Dec 2006 5153 – 5767
- [11] T. Chudoba, M. Griepentrog, A. Dück, D. Schneider, F. Richter, J. Mater. Res., 19 (2004) 301
- [12] N. Schwarzer, (2007) "Intrinsic stresses – Their influence on the yield strength and their measurement via nanoindentation", online archives of the Saxonian Institute of Surface Mechanics www.siomec.de/pub/2007/001
- [13] N. Schwarzer, "Modelling of Contact Problems of Rough Surfaces", online archives of the Saxonian Institute of Surface Mechanics www.siomec.de/pub/2007/007
- [14] FilmDoctor: Software demonstration package, www.siomec.de/FilmDoctor